Applied Catalysis B: Environmental 181 (2016) 716–726

Contents lists available at ScienceDirect

Applied Catalysis B: Environmental

journal homepage: www.elsevier.com/locate/apcatb

Rhodium(0) nanoparticles supported on nanosilica: Highly active and long lived catalyst in hydrogen generation from the methanolysis of ammonia borane

Derya Özhava, Saim Özkar*

Department of Chemistry, Middle East Technical University, 06800 Ankara, Turkey

ARTICLE INFO

Article history:
Received 23 April 2015
Received in revised form 16 August 2015
Accepted 24 August 2015
Available online 5 September 2015

Keywords:
Hydrogen generation
Ammonia borane
Methanolysis
Silica nanopowder
Rhodium(0)
Nanoparticles

ABSTRACT

Nanosilica stabilized rhodium(0) nanoparticles (Rh(0)/nanoSiO$_2$), *in situ* formed from the reduction of rhodium(II) octanoate impregnated on the surface of nanosilica, are active catalyst in hydrogen generation from the methanolysis of ammonia borane at room temperature. Monitoring the hydrogen evolution enables us to follow the kinetics of nanoparticles formation. The resulting sigmoidal kinetic curves are analyzed by using the 2-step mechanism of the slow, continuous nucleation and autocatalytic surface growth. By using the temperature dependent kinetic data, we could calculate the activation energy for the nucleation and autocatalytic surface growth of rhodium(0) nanoparticles as well as for the catalytic methanolysis of ammonia borane. Rh(0)/nanoSiO$_2$ could be isolated and characterized by a combination of advanced analytical techniques including XRD, TEM, EDX, XPS, and N_2 adsorption–desorption. The results reveal that rhodium(0) nanoparticles are highly dispersed on nanosilica surface and have tunable particle size depending on the initial metal concentration. An increase in the mean particle size of rhodium(0) nanoparticles is observed when the initial metal concentration increases. Rh(0)/nanoSiO$_2$ are highly active and long lived catalyst in hydrogen generation from the methanolysis providing an exceptional initial turnover frequency of TOF = 168 min^{-1} (504 min^{-1} corrected for the surface atoms) at 25.0 ± 0.5 °C, which is the highest value ever reported for rhodium catalysts. An inverse dependence of TOF on the initial rhodium concentration is observed and ascribed to the increasing size of rhodium(0) nanoparticles. Carbon disulfide poisoning and filtration experiments unequivocally demonstrate that rhodium(0) nanoparticles are the true heterogeneous catalyst in hydrogen generation from the methanolysis of ammonia borane.

1. Introduction

In the face of a growing global population and economy, the energy demand is ever rising. In order to fulfill this energy demand while also reducing both consumption of fossil fuels and emission of greenhouse gases, there is urgent need to supplement energy feedstocks with renewable sources [1,2]. Hydrogen provides tremendous promises as clean energy vector on the way towards a sustainable energy future [3,4]. However, the main obstacle on the way to a hydrogen powered society is the efficient storage and release of hydrogen under ambient conditions [5]. In recent years, intensive efforts have been devoted to developing safe and efficient methods for hydrogen storage. Ammonia borane (NH_3BH_3, AB) appears to be potential hydrogen storage materials due to its high hydrogen content (19.6% wt.), high stability, and nontoxicity [6]. In general, release of hydrogen stored in AB can be achieved through thermal degradation in solid state or solvolysis (hydrolysis or methanolysis) in solution [7,8,9]. Hydrolysis of AB in aqueous medium is widely accepted and well-studied because of favorable kinetics and mild reaction conditions [10,11]. Nevertheless, the concomitant release of ammonia in applications with high concentration of AB and difficulties in recycling process of hydrolysis product, ammonium metaborate (NH_4BO_2), are the

Abbreviations: AB, ammonia borane; Rh^{2+}, rhodium(II) ion; Rh(0), rhodium(0); nanosilica, silica nanopowder; Rh(0)/nanoSiO$_2$, nanosilica stabilized rhodium(0) nanoparticles; TEM, transmission electron microscopy; EDX, energy dispersive X-ray spectroscopy; XRD, X-ray diffraction; XPS, X-ray photoelectron spectroscopy.

* Corresponding author. Fax: +90 312 210 3200.
E-mail address: sozkar@metu.edu.tr (S. Özkar).

http://dx.doi.org/10.1016/j.apcatb.2015.08.038
0926-3373/

most frequently encountered problems in using the hydrolysis of AB for hydrogen generation [12]. Ramachandran and co-workers have demonstrated how to eliminate both of these drawbacks by using methanol as solvent; pure hydrogen gas is released from catalytic methanolysis of AB and also the methanolysis product, ammonium tetramethoxyborate, can be converted back to AB by a room temperature process with $LiAlH_4$ plus NH_4Cl [8]. The methanolysis of AB can release 3.0 equivalents of H_2 per mole of AB only in the presence of a suitable catalyst (Eq. (1)):

$$NH_3BH_3 + 4CH_3OH \xrightarrow{catalyst} NH_4B(OCH_3)_4 + 3H_2 \quad (1)$$

Up to now, a number of heterogeneous catalysts have been investigated to accelerate the methanolysis of AB, such as $RuCl_3$, $RhCl_3$, $PdCl_2$, $CoCl_2$, $NiCl_2$ [8], copper nanoparticles [13], polymer stabilized-nickel(0) [14], -palladium(0) [15], and -ruthenium(0) nanoparticles [16], Co-Co_2B, Ni-Ni_3B, Co-Ni-B [17], zeolite confined rhodium(0) nanoparticles [18], MMT-immobilized ruthenium(0) nanoparticles [19], cobalt-palladium nanoparticles [20], mesoporous CuO nanostructures [21], Cu-Cu_2O-CuO/C [22]. Although transition metal nanoparticles are of great importance in the methanolysis of AB owing to their high catalytic activity, they have tendency to aggregation and, therefore, relatively short lifetime [23]. Metal nanoparticles have been stabilized against agglomeration in order to retain their large surface area, high activity, and long lifetime by using microporous or mesoporous materials as well as oxide supports with large surface area [24–26]. Among these materials, silica has been widely used because of low cost, wide accessibility, high thermal stability, excellent porosity, and high surface reactivity [27,28]. Reducing the particle size of support from the microcrystalline to the nanocrystalline regime (from >1 μm to <100 nm) can enhance the catalytic activity of the supported materials due to increase in the external surface area of support [29].

Herein we report the use of nanosilica with an average particle size of 12 nm for the stabilization of rhodium(0) nanoparticles which are highly active catalyst in hydrogen generation from the methanolysis of ammonia borane. Nanosilica stabilized rhodium(0) nanoparticles, hereafter referred to as Rh(0)/nanoSiO_2, were *in situ* formed from the reduction of rhodium(II) ions impregnated on nanosilica during the methanolysis of AB in methanol. Both impregnation of rhodium(II) ions on nanosilica matrix and reduction of rhodium(II) ions to rhodium(0) by AB were carried out in the same reaction flask. Performing the impregnation of rhodium(II) ions and, then the *in situ* formation of Rh(0)/nanoSiO_2 in the same medium provides opportunity to avoid laborious catalyst preparation steps. Rh(0)/nanoSiO_2 were separated from the reaction solution and characterized by TEM, TEM-EDX, XRD, XPS, and N_2-adsorption/desorption techniques. This work also comprises the following major findings: (i) formation of homogeneously distributed rhodium(0) nanoparticles in the pores of nanosilica matrix with a mean particle size in the range of 3.4–4.9 nm depending on the initial concentration of precursor compound, (ii) the use of Rh(0)/nanoSiO_2 as catalyst in hydrogen generation from the methanolysis of AB, (iii) the kinetics of the catalytic reaction, (iv) the 2-step formation kinetics of rhodium(0) nanoparticles during the methanolysis of AB by using the hydrogen generation as reporter reaction, (v) determination of activation energy for the nucleation and autocatalytic surface growth of rhodium(0) nanoparticles as well as for the catalytic methanolysis of AB, (vi) remarkable catalytic activity of Rh(0)/nanoSiO_2 in hydrogen generation from the methanolysis of AB with an initial turnover frequency of TOF = 168 min^{-1} (504 min^{-1} corrected for the surface atoms) at 25.0 ± 0.5 °C.

2. Experimental

2.1. Materials

Rhodium(II) octanoate dimer ($[Rh(C_7H_{15}CO_2)_2]_2$), ammonia borane (H_3NBH_3, 97%), methanol (99%), and silica nanopowder (SiO_2, particle size ≈ 12 nm) were purchased from Aldrich. Nanosilica was dried in vacuum at 120 °C and stored under N_2 atmosphere. Methanol was distilled over metallic magnesium and stored under inert gas atmosphere. Distilled methanol was used in all methanolysis reactions under inert gas atmosphere unless otherwise specified. All glassware was cleaned with acetone, followed by copious rinsing with distilled water before drying in an oven at 120 °C.

2.2. Instrumentation

Transmission electron microscopy (TEM) was performed on a JEM-2100F (JEOL) microscope operating at 200 kV. The TEM samples were harvested from *in situ* generated Rh(0)/nanoSiO_2 solution at the end of catalytic methanolysis of AB. A few drops of nanoparticle solution was redispersed in 2 mL methanol and ultrasonicated for 3 min. Holey carbon coated copper grid was dipped in colloidal solution for a few seconds, then removed and dried under inert atmosphere. Samples were examined at magnification between 100 and 400 K. The samples used for XPS, XRD or N_2 adsorption desorption analysis were harvested from *in situ* generated Rh(0)/nanoSiO_2 solution at the end of catalytic methanolysis of AB. The catalyst solution was connected to vacuum and dried after methanolysis of AB. The X-ray photoelectron spectroscopy (XPS) analysis was performed on a Physical 15 Electronics 5800 spectrometer equipped with a hemispherical analyzer and using monochromatic Al Kα radiation of 1486.6 eV, the X-ray tube working at 15 kV, 350 W and pass energy of 23.5 keV. The X-ray diffraction (XRD) pattern was recorded on a MAC Science MXP 3TZ diffractometer using Cu-Kα radiation (wavelength 1.5406 Å, 40 kV, 55 mA). NMR spectra were recorded on a Bruker Avance DPX 400 MHz spectrometer (400.1 MHz for ^1H; 128.3 MHz for ^{11}B). $BF_3{\cdot}(C_2H_5)_2O$ was used as external reference for ^{11}B NMR chemical shifts. The nitrogen adsorption/desorption experiments were carried out at 77 K using a NOVA 3000 series Quantachrome Instrument. The sample was out gassed under vacuum at 573 K for 3 h before the adsorption of nitrogen.

2.3. In situ *preparation of Rh^{+2}–ion impregnated on nanosilica surface (Rh^{+2}/nanoSiO_2)*

A stock solution of 4.9 mM Rh^{+2} was prepared by dissolving 47.8 mg (0.123 mmol Rh) rhodium(II) octanoate dimer in about 10 mL methanol in a 25.0 mL volumetric flask and by adding more methanol to get 25.0 mL volume. Certain aliquot of this stock solution was transferred into the reaction flask containing nanosilica powder. For instance, for the preparation of a 0.49 mM Rh precatalyst mixture, 1.0 mL (4.9 μmol Rh) aliquot of stock solution is transferred into reaction flask containing 50 mg nanosilica powder which corresponds to a rhodium loading of 1.0 wt.% Rh. After addition of 6.0 mL methanol with a glass pipette, the resulting suspension was stirred for 3 h to ensure complete adherence of Rh^{+2} ions to the support at 25.0 ± 0.5 °C.

2.4. In situ *formation of Rh(0)/nanoSiO_2 and catalytic methanolysis of AB*

The *in situ* formation of Rh(0)/nanoSiO_2 and concomitant hydrogen generation from the methanolysis of AB were achieved in the same reaction flask (Fig. 1). The catalytic activity of Rh(0)/nanoSiO_2

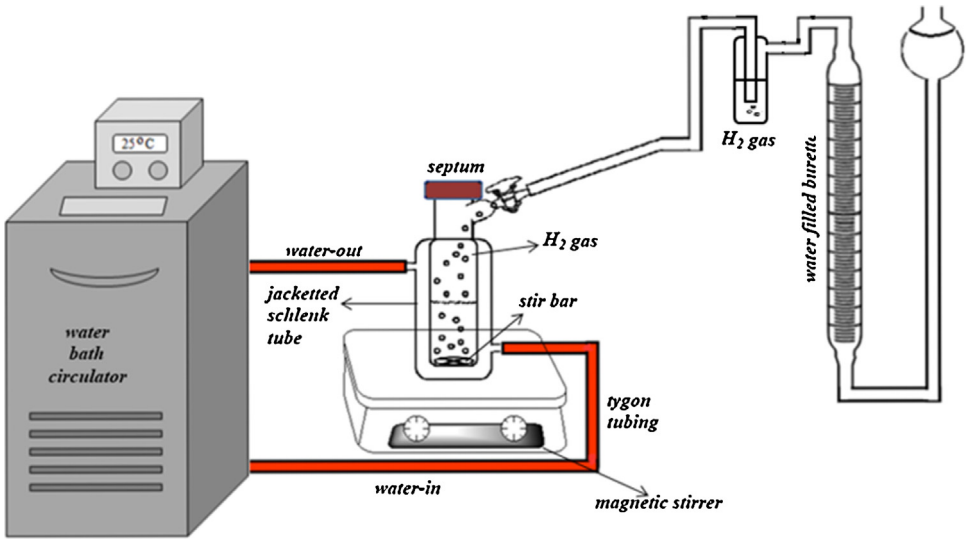

Fig. 1. An illustration of experimental set up used for performing the catalytic methanolysis of ammonia borane at constant temperature and measuring the hydrogen generated from the reaction.

in the methanolysis of AB was determined by following the liberation of hydrogen gas. The experiment was performed as follows: a jacketed 50 mL reaction flask with a Teflon-coated stir bar is first evacuated to remove any trace of oxygen and moisture present and then filled with nitrogen inert gas. The reaction flask is thermostated by circulating water through its jacket at 25.0 ± 0.5 °C or at a certain temperature specified. The gas outlet of the reaction flask is connected to a graduated glass tube filled with water through a bubbler containing 20 mL of methylcyclohexane (Fig. 1). In a typical experiment, a solution of 64 mg (2.0 mmol) AB in 3.0 mL methanol is added *via* a gastight syringe to the reaction flask containing 7.0 mL suspension of Rh^{+2}/nanoSiO_2 in methanol with the desired Rh^{+2} concentration and the catalytic methanolysis of AB is launched. After a short induction time, the color changes from pale blue to black indicating the formation of rhodium(0) nanoparticles in methanol solution and rapid hydrogen generation from methanolysis of AB starts. The volume of hydrogen evolved during catalytic methanolysis is recorded by measuring the displacement of water level in the glass tube at constant pressure. When no more hydrogen liberated, experiment is stopped.

The average number of rhodium atoms in the $Rh(0)_{\sim n}$ nanoparticles was estimated from the average particle size obtained by TEM images on the basis of an assumed cubic structure for rhodium: $n = (N0\rho(4/3)\pi(D/2)^3)/W$ [30], where n = number of Rh atoms, $N0 = 6.022 \times 10^{23}$ mol^{-1}, ρ = density of rhodium at room temperature (12.41 g/cm^3), D = diameter of rhodium nanoparticles, and W = atomic weight of rhodium (102.91 g/mol), r = atomic radius of rhodium (135 pm) [31].

2.5. Activation parameters for the methanolysis of AB catalyzed by Rh(0)/nanoSiO_2

In order to determine the activation parameters, catalytic methanolysis of 200 mM (64 mg) AB was performed starting with 50 mg Rh^{+2}/nanoSiO_2 (1.0 wt.% Rh, 0.49 mM Rh) at various temperatures. For each temperature, the value of rate constant, k_{obs}, was calculated from the hydrogen generation rate and used to determine the activation energy (E_a) by using Arrhenius plot as well as the enthalpy change of activation ($\Delta H^{\neq}$) and the entropy change of activation ($\Delta S^{\neq}$) by drawing Eyring–Polanyi plot.

2.6. Catalytic lifetime of Rh(0)/nanoSiO_2 catalyst in the methanolysis of AB

The lifetime of the catalyst was measured by determining the total turnover number (TTON) of hydrogen generation from the methanolysis of AB catalyzed by Rh(0)/nanoSiO_2. For this purpose, lifetime experiment was started with 10 mL solution containing 50 mg Rh^{+2}/nanoSiO_2 (2.0 wt.% rhodium, 9.9 μmol Rh) and 400 mM (128 mg) AB at 25.0 ± 0.5 °C. When the expected amount of hydrogen evolved, a new batch of substrate was added to the reaction medium under nitrogen inert gas. Same procedure was applied until no more hydrogen liberation was observed.

2.7. Heterogeneity test for Rh(0)/nanoSiO_2 by carbon disulfide poisoning in the methanolysis of AB

In order to test the heterogeneity of nanosilica stabilized rhodium(0) nanoparticles, catalyst poisoning experiment was performed by using carbon disulfide (CS_2) as poison. Firstly, a 2.0 mM stock solution of CS_2 was prepared in 10 mL methanol. Then, a typical methanolysis reaction of AB catalyzed by Rh(0)/nanoHAP was initiated with 50 mg Rh^{+2}/nanoSiO_2 (1.0% wt. Rh, 0.49 mM Rh) and 200 mM AB at 25.0 ± 0.5 °C. At the time when about 40% of hydrogen evolved, 0.5 mL (0.2 μmol) CS_2 solution was added to reaction medium *via* a gastight syringe in order to poison the catalyst. Hydrogen generation ceased immediately upon the addition of CS_2 solution and the reaction was followed for 10 min to observe no further hydrogen evolved.

2.8. Leaching test for Rh(0)/nanoSiO_2

After the first run of catalytic methanolysis of 200 mM AB, catalyzed by 50 mg Rh(0)/nanoSiO_2 (1.0% wt. Rh, 0.49 mM Rh), the reaction was stopped and opened under nitrogen inert gas atmosphere and the suspension in reaction flask was filtered; the filtrate was transferred in another reaction flask, and 64.0 mg AB (200 mM AB) was added. The hydrogen generation from methanolysis of AB was followed as described above. No hydrogen generation was observable in 2 h indicating that the filtrate has no catalytic activity in the methanolysis of AB; thus no leaching of rhodium into the solution could be detected.

3. Results and discussion

3.1. In Situ *formation of Rhodium(0) nanoparticles during the methanolysis of AB*

The formation of nanosilica stabilized rhodium(0) nanoparticles, hereafter referred to as Rh(0)/nanoSiO$_2$, and hydrogen generation from the methanolysis of AB were achieved in the same medium. Rh(0)/nanoSiO$_2$ was obtained from the reduction of rhodium(II) octanoate impregnated on the porous nanosilica, Rh^{+2}/nanoSiO$_2$, during the methanolysis of AB at room temperature. When AB solution is added to the reaction flask containing a suspension of Rh^{+2}/nanoSiO$_2$ precatalyst in methanol, the reduction of rhodium(II) ions and hydrogen evolution from the methanolysis of AB start at the same time. The formation of rhodium(0) nanoparticles and concomitant hydrogen generation from the methanolysis of AB are followed by monitoring the volume of H_2 liberated and, then converting into the equivalent H_2 per mole of AB, using the known 3:1 H_2/AB stoichiometry (Eq. (1)). Fig. 2 depicts the plots of mol H_2 evolved per mole of AB *versus* time for the catalytic methanolysis of AB starting with 200 mM AB and 50 mg of Rh^{+2}/nanoSiO$_2$ (1.0 wt.% Rh, [Rh] = 0.49 mM) in 10 mL methanol at 25.0 ± 0.5 °C. After an induction time of 1.5 min, the color of the solution changes from pale blue to black, hydrogen release launches immediately and continues almost linearly until the complete conversion of ammonia borane to ammonium tetramethoxyborate as seen by the signal at 8.7 ppm[8] in the ^{11}B NMR spectrum in Fig. 3. The color change and the sigmoidal shape of hydrogen generation curve indicate the reduction of rhodium(II) ions and formation of rhodium(0) nanoparticles with a two-step, nucleation and autocatalytic growth mechanism of nanoparticle formation [32,33].

A comparative study was carried out starting with rhodium(II) octanoate either alone or impregnated on the nanosilica to demonstrate the effect of support on the activity and stability of rhodium(0) nanoparticles formed under the same conditions. Fig. 4

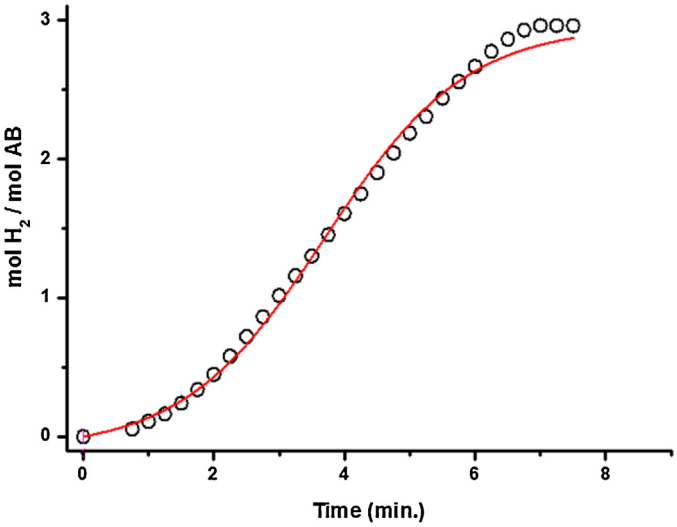

Fig. 2. Plots of mol H_2 evolved per mole of AB *versus* time for the catalytic methanolysis of AB starting with 200 mM AB and 50 mg of Rh^{+2}/nanoSiO$_2$ (1.0 wt.% Rh, [Rh] = 0.49 mM) in 10 mL methanol at 25.0 ± 0.5 °C.

shows the plots of mole H_2 evolved per mole of AB *versus* time for the catalytic methanolysis of AB starting with 200 mM AB plus either 50 mg of Rh^{+2}/nanoSiO$_2$ (1.0 wt.% Rh, [Rh] = 0.49 mM) or 1.9 mg of rhodium(II) octanoate (0.49 mM Rh) in 10 mL methanol at 25.0 ± 0.5 °C. Although both catalysts show similar initial activity in hydrogen generation from the methanolysis of AB, the rhodium(0) nanoparticles in the absence of support lose catalytic activity rapidly. Furthermore, in the case of using rhodium(II) octanoate without support one observes bulk rhodium metal precipitate at the end of methanolysis. Hence, it can be concluded that rhodium(0) nanoparticles are not stable in the absence of support and do aggregate to bulk metal. Therefore, nanosilica support is

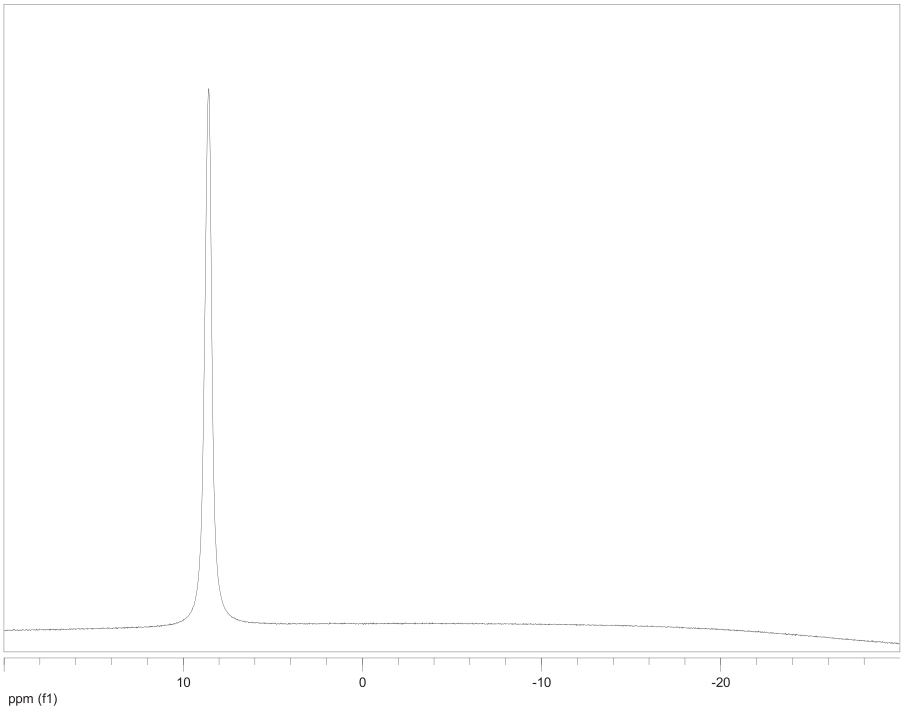

Fig. 3. ^{11}B NMR spectrum taken at the end of catalytic methanolysis of AB starting with 200 mM AB and 50 mg of Rh^{+2}/nanoSiO$_2$ (1.0 wt.% Rh, [Rh] = 0.49 mM) in 10 mL methanol at 25.0 ± 0.5 °C.

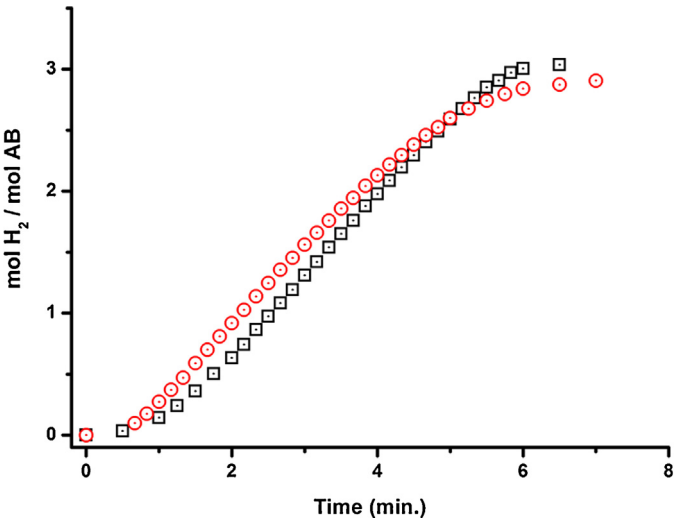

Fig. 4. Plots of mol H_2 evolved per mole of AB *versus* time for the catalytic methanolysis of AB starting with 200 mM AB plus either (black squares, □) 50 mg of $Rh^{+2}/nanoSiO_2$ (1.0 wt.% Rh, [Rh] = 0.49 mM) or (red circles, ○) 1.9 mg of rhodium(II) octanoate (0.49 mM Rh) in 10 mL methanol at 25.0 ± 0.5 °C.(For interpretation of the references to color in this figure legend, the reader is referred to the web version of this article.)

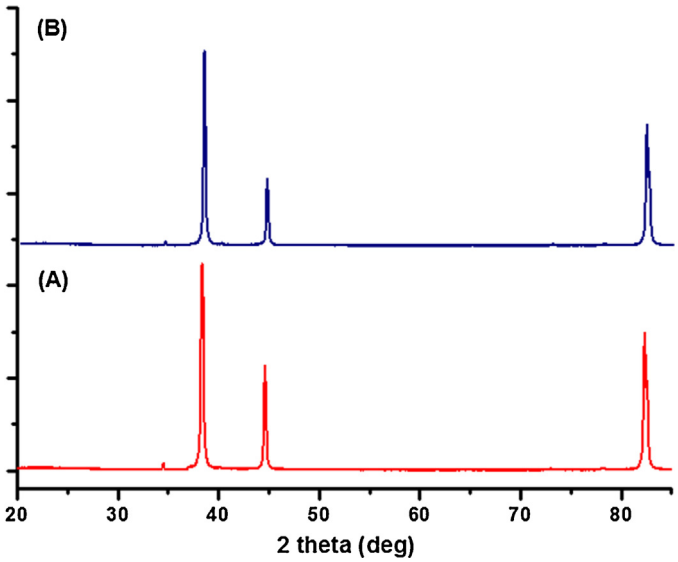

Fig. 5. Powder X-ray diffraction (PXRD) patterns of (A) silica nanopowder ($nanoSiO_2$), (B) nanosilica stabilized rhodium(0) nanoparticles ($Rh(0)/nanoSiO_2$) with rhodium loading of 3.0% wt. Rh.

required for obtaining rhodium(0) nanoparticles which are stable and yet catalytically active.

The formation kinetics of rhodium(0) nanoparticles catalyst can be acquired using hydrogen evolution as reporter reaction [32–34]. The Finke–Watzky 2-step mechanism (nucleation and autocatalytic growth) for the nanoparticle formation [34] is given in Scheme 1, where P stands for the added precursor $Rh^{+2}/nanoSiO_2$ and Q for the growing $Rh(0)_n$ nanoparticles.

Kinetics of the $Rh(0)_n$ nanoparticle formation can be obtained from the fit of hydrogen evolution data to the 2-step mechanism if the rate of hydrogen generation is fast in comparison to the rate of nanoparticle formation. Sigmoidal kinetics curve observed in Fig. 2 fit well to the function given in Eq. (2) [34].

$$[AB]_t = [AB]_o - \frac{k_1/k_2 + [AB]_o}{1 + k_1/k_2[AB]_o \exp(k_1 + k_2[AB]_0)t} \quad (2)$$

Here, k_1 is the rate constant for the slow, continuous nucleation, k_2 is the rate constant for the autocatalytic surface growth, $[AB]_o$ and $[AB]_t$ are the concentration of AB at time 0 and t, respectively. The observation of sigmoidal dehydrogenation curve and its curve-fit to the slow, continuous nucleation, followed by autocatalytic surface growth kinetics are very strong evidence for the formation of rhodium(0) nanoparticles catalyst from a soluble precursor complex in the presence of reducing agent. The rate constants obtained from the nonlinear least square curve-fit in Fig. 2 are $k_1 = 3.0 \times 10^{-2}$ min^{-1} and $k_2 = 1.2 \times 10^2$ M^{-1} min^{-1} (k_2 has been corrected mathematically for stoichiometry factor of 407 as described elsewhere [34], but not for the "scaling factor"; it means that this correction is not related to the changing the number of rhodium atoms on the growing surface of metal). These rate constants are for the continuous slow nucleation and autocatalytic surface growth reaction of rhodium(0) nanoparticles, respectively, starting with 200 mM AB and 50 mg of $Rh^{+2}/nanoSiO_2$ (1.0 wt.% Rh, [Rh] = 0.49 mM) in 10 mL methanol at 25.0 ± 0.5 °C. It is noteworthy that since k_1 and k_2 are the rate constants of two different reactions there exists no direct correlation between them.

$$P \xrightarrow{k_1} Q$$

$$P + Q \xrightarrow{k_2} 2Q$$

$$H_3NBH_3\,(aq) + 4CH_3OH\,(l) \xrightarrow{Q\,(fast)} NH_4^+(aq) + B(OCH_3)_4^-(aq) + 3H_2(g)$$

Scheme 1. Illustration of the methanolysis of AB as reporter reaction: P is the precursor rhodium(II) ions impregnated on the porous nanosilica and Q is the growing $Rh(0)_n$ nanoparticles catalyst.

3.2. Characterization of $Rh(0)/nanoSiO_2$

The $Rh(0)/nanoSiO_2$, *in situ* formed from the reduction of $Rh^{+2}/nanoSiO_2$ precatalyst during methanolysis of AB at room temperature, was isolated from the reaction solution by centrifugation and characterized by using a combination of advanced analytical techniques. Fig. 5 depicts XRD patterns of silica nanopowder ($nanoSiO_2$) and nanosilica stabilized rhodium(0) nanoparticles ($Rh(0)/nanoSiO_2$) which show that there is no observable change in intensities or in the positions of the main Bragg peaks of silica. This specifically indicates that both crystallinity and the lattice of nanosilica remain intact after the preparation of $Rh^{+2}/nanoSiO_2$ and the reduction of rhodium(II) to rhodium(0) during the methanolysis of AB. No additional peak is observable for rhodium(0) nanoparticles due to the low loading of nanosilica sample.

The morphology and particle size of nanosilica stabilized rhodium(0) nanoparticles were examined by TEM. Fig. 6 illustrates the TEM images of nanosilica stabilized rhodium(0) nanoparticles with different rhodium loading (0.50, 1.0, 2.0, 3.0, and 5.0% wt. Rh) harvested after catalytic methanolysis reaction which show the existence of rhodium(0) nanoaparticles uniformly dispersed on the surface of nanosilica. Fig. 6f shows the plot of particle size of rhodium(0) nanoparticles *versus* the rhodium loading (% wt.) of $Rh(0)/nanoSiO_2$ samples. Expectedly, the particle size increases as the rhodium percentage of the sample increases.

The nanosilica stabilized rhodium(0) nanoparticles were analyzed by X-Ray photoelectron spectroscopy for the chemical composition of materials and oxidation state of rhodium. The survey scan spectrum of $Rh(0)/nanoSiO_2$ with a rhodium loading of 5.0% wt. Rh (Fig. 7a) shows the existence of rhodium as the only element detected in addition to the framework elements of silica (Si and O). Fig. 7b demonstrates the high resolution Rh 3d XPS spectrum of the same $Rh(0)/nanoSiO_2$ sample. Two prominent bands observed at 306.7 and 311.8 eV can be ascribed to Rh(0) $3d_{5/2}$ and Rh(0) $3d_{3/2}$, respectively, by comparison to the values of metallic

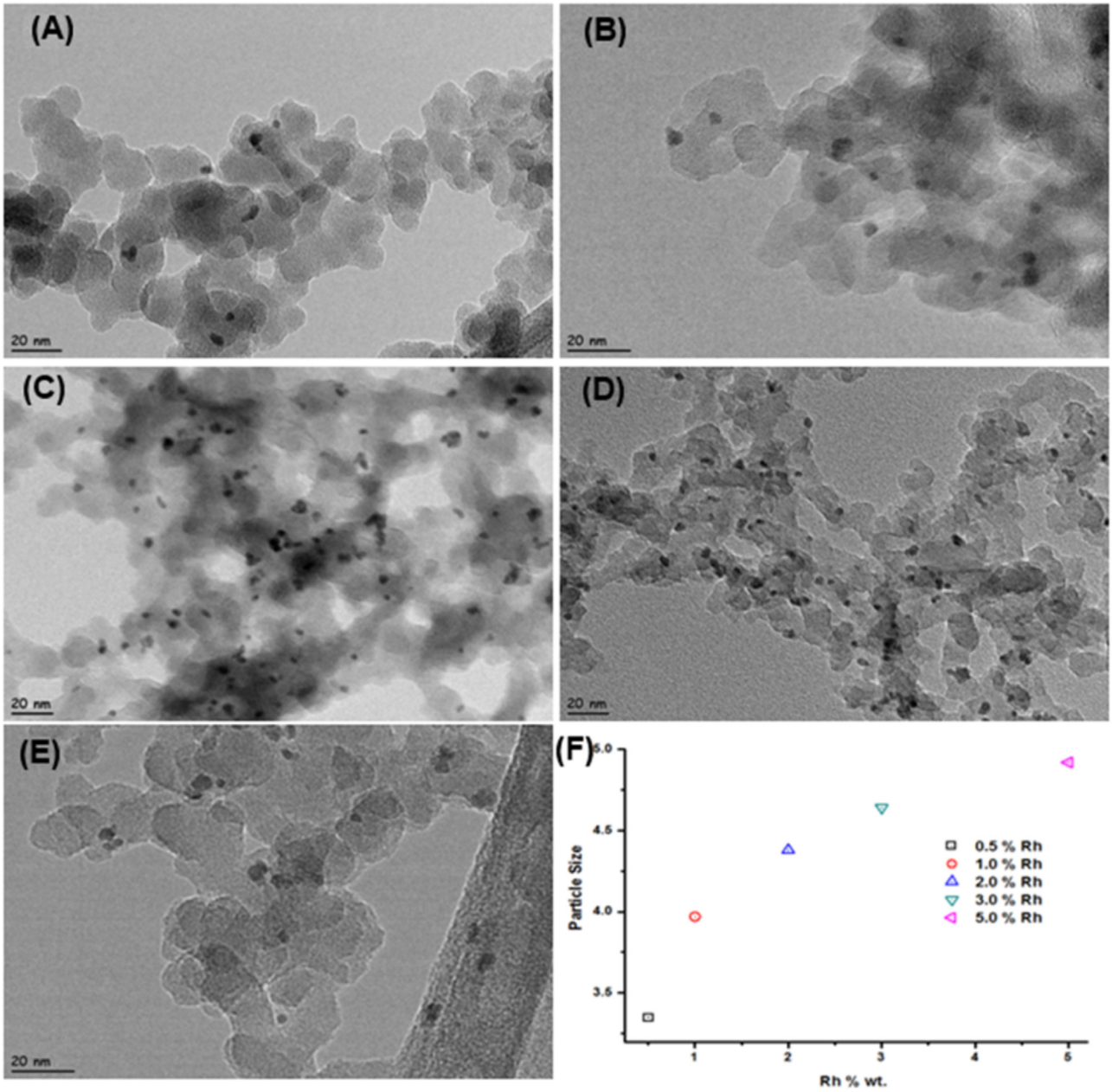

Fig. 6. TEM images of nanosilica stabilized rhodium(0) nanoparticles with different rhodium loading (A) 0.5, (B) 1.0, (C) 2.0, (D) 3.0 and (E) 5.0% wt. Rh after catalytic methanolysis reaction performed starting with 200 mM AB catalyzed by desired amount of nanosilica stabilized Rh(0) nanoparticles at 25.0 ± 0.5 °C. (F) the plot of percentage rhodium loading *versus* particle size.

rhodium [35,36]. Two additional higher energy peaks at 309.1 and 314.8 eV show the presence of rhodium in higher oxidation state, likely in the form of oxide [37,38], which may arise from the oxidation of rhodium(0) nanoparticles when exposed to air for a few minutes during XPS sampling.

BET surface areas of nanoSiO$_2$ and Rh(0)/nanoSiO$_2$ with a rhodium loading of 5.0% wt. Rh were calculated to be 246.8 and 282.4 m^2 g^{-1}, respectively. The increase by 35.6 m^2 g^{-1} in the surface area on passing from nanoSiO$_2$ to Rh(0)/nanoSiO$_2$ is another piece of evidence for the presence of rhodium(0) nanoparticles on the surface of nanosilica.

3.3. Catalytic activity of Rh(0)/nanoSiO$_2$ in the methanolysis of AB

Nanosilica stabilized rhodium(0) nanoparticles, *in situ* formed from the reduction of rhodium(II) octanoate impregnated on the surface of porous nanosilica, are active catalyst in hydrogen generation from the methanolysis of AB even in low catalyst concentrations at room temperature. Fig. 8a depicts the plots of equivalent H_2 evolved per mole of AB *versus* time during the catalytic methanolysis performed starting with 200 mM AB in various rhodium loading, thus in various rhodium concentration at 25.0 ± 0.5 °C. In all of these experiments, hydrogen generation starts immediately after a short induction period and continues linearly until 3.0 equivalent hydrogen evolved. That the catalytic activity remains unchanged during the surface growth of rhodium(0) nanoparticles indicates the structure insensitivity of the methanolysis reaction. All the experimental curves have the sigmoidal shape and fit well to the two-step mechanism [32], which enables us to determine the rate constants k_1 of the slow, continuous nucleation and k_2 of the autocatalytic surface growth for the formation of rhodium(0) nanoparticles catalyst from rhodium(II)

Table 1
The rate constants k_1 of the slow, continuous nucleation, P → Q, and k_2 of the autocatalytic surface growth, P + Q → 2Q, for the formation of rhodium(0) nanoparticles catalyst from the reduction of rhodim(II) ions during the methanolysis of AB (200 mM) starting with Rh^{+2}/nanoSiO_2 with different rhodium loading, rhodium concentrations, hydrogen generation rates, turnover frequency (TOF) values, and the TOF values corrected for the number of rhodium atoms on the surface of nanoparticles for the methanolysis of AB at 25.0 ± 0.5 °C.

wt. %Rh	Particle size (nm)	Number of Rh atoms in NP	Number of Rh atoms on surface	[Rh] (mM)	k_1 (min^{-1})	k_2 (M^{-1} min^{-1})	k_2/k_1	H_2 generation rate (mmol min^{-1})	TOF (min^{-1})	$TOF_{corrected}$ (min^{-1})
0.50	3.4 ± 0.4	1494	498	0.24	$(3.35 \pm 0.16) \times 10^{-2}$	97.8 ± 3.1	2.92×10^3	0.55	168	504
1.0	4.0 ± 1.0	2432	689	0.49	$(3.03 \pm 0.24) \times 10^{-2}$	121.1 ± 3.9	4.00×10^3	1.17	147	519
2.0	4.4 ± 0.7	3237	834	0.99	$(3.26 \pm 0.38) \times 10^{-2}$	124.2 ± 4.6	3.81×10^3	2.38	133	516
3.0	4.6 ± 1.1	3699	911	1.5	$(3.33 \pm 0.36) \times 10^{-2}$	115.7 ± 3.7	3.47×10^3	3.37	119	483
5.0	4.9 ± 1.8	4471	1034	2.5	$(4.11 \pm 0.64) \times 10^{-2}$	97.2 ± 4.2	2.37×10^3	5.24	108	467

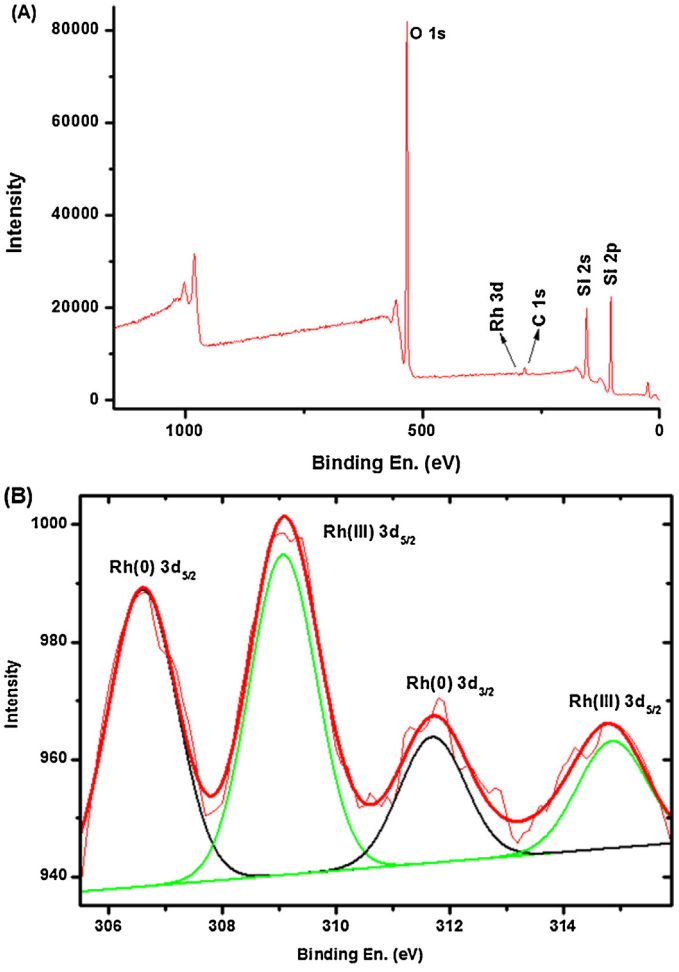

Fig. 7. (A) X-ray photoelectron (XPS) survey scan spectrum, (B) high resolution Rh 3d XPS spectrum of Rh(0)/nanoSiO_2 with a rhodium loading of 5.0% wt. Rh.

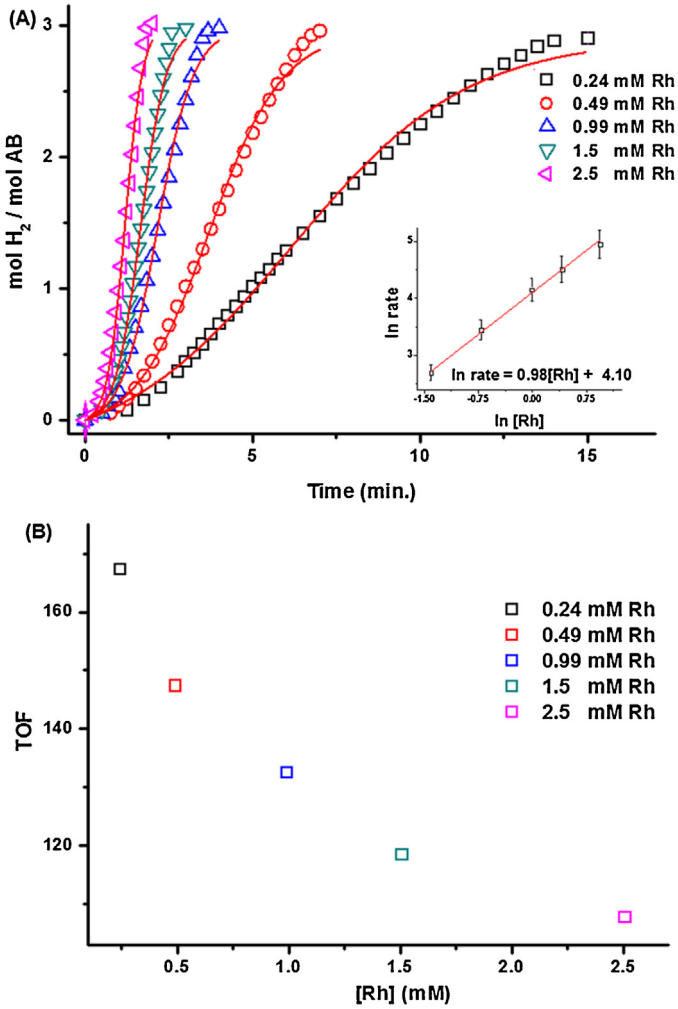

Fig. 8. (A) Plots of mole H_2 evolved per mole of AB *versus* time for methanolysis of 200 mM AB in different metal concentrations ([Rh] = 0.22, 0.49, 0.99, 1.5, 2.5 mM, each prepared using metal loading of 0.50, 1.0, 2.0, 3.0, 5.0% wt. Rh, respectively) at 25.0 ± 0.5 °C. Inset: Plot of hydrogen generation rate *versus* the concentration of rhodium (both in logaritmic scale.). (B) Inverse dependence of initial TOF value on the initial precatalyst Rh concentration.

ions during the methanolysis of AB (Table 1) [34]. The large value of k_2/k_1 (Table 1) indicates high level of kinetic control for the rhodium(0) nanoparticles formation from the reduction of rhodium(II) ion.

The hydrogen generation rate was determined from the linear portion of each plot in Fig. 8a and converted to the turnover frequency (TOF) of rhodium(0) nanoparticles in hydrogen generation from the methanolysis of AB at 25.0 ± 0.5 °C. The TOF values, defined per rhodium present in the catalyst as usual [39], as well as TOF values corrected for the number of rhodium atoms on the surface of nanoparticle, and hydrogen generation rates for the methanolysis of AB in different initial concentration of rhodium at 25.0 ± 0.5 °C were also listed in Table 1. Rh(0)/nanoSiO_2 sample with rhodium loading of 0.5 wt.% Rh provides the highest catalytic activity with an initial TOF = 168 min^{-1} (504 min^{-1} corrected for surface rhodium atoms, Table 1) ever reported for hydrogen generation from the methanolysis of AB at 25.0 ± 0.5 °C.

Turnover frequency decreases with the increasing initial concentration of rhodium in the Rh(0)/nanoSiO_2 catalyst, down to a value of 108 for the 5.0% wt. Fig. 5b shows the inverse dependence of the TOF on the initial concentration of precatalyst. Understanding this inverse dependence of the TOF on precatalyst concentration is

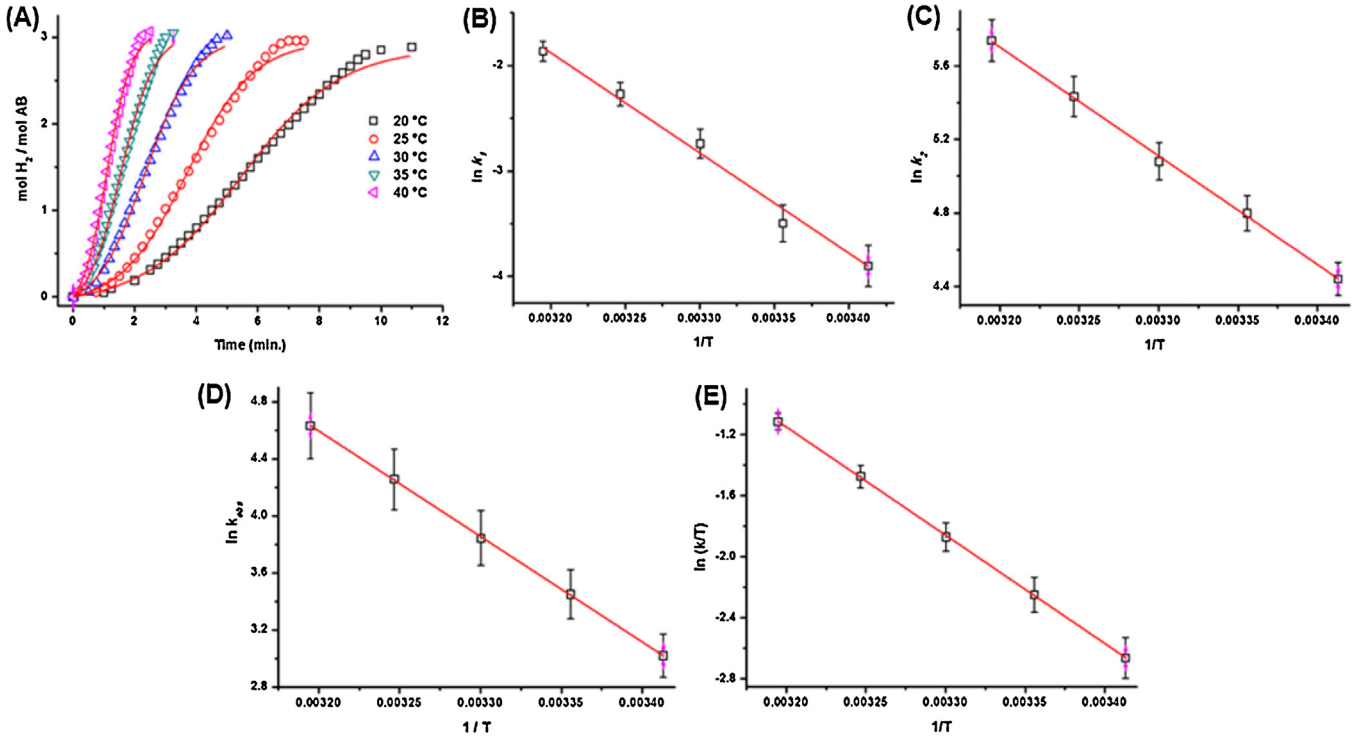

Fig. 9. (A) Plots of mole H_2 evolved per mole of AB *versus* time for the catalytic methanolysis of AB at various temperatures in the range of 20–40 °C keeping the concentration of substrate at [AB] = 200 mM and rhodium at [Rh] = 0.49 mM (1.0 wt.% Rh, 50 mg Rh(0)/nanoSiO$_2$), (B) The Arrhenius plot for nucleation of rhodium(0) nanoparticles, (C) The Arrhenius plot for the autocatalytic surface growth of rhodium(0) nanoparticles, (D) The Arrhenius plot, (E) The Eyring plot for Rh(0)/nanoSiO$_2$ catalyzed methanolysis of AB. [AB] = 200 mM, [Rh] = 0.49 mM (1.0 wt.% Rh, 50 mg Rh(0)/nanoSiO$_2$).

important since the true TOF should be constant for a given metal containing catalyst in a given reaction under specified reaction conditions [40]. In literature the inverse dependencies of TOF on the catalyst concentration have been reported many times [41–47] along with some explanation. One of the mechanisms suggested for the observed inverse relation between the TOF and catalyst concentration correlates the variation in the catalytic activity with the particles size in size specific reactions [48]. The use of lower concentration of precatalyst forms smaller particles and higher catalytic activity is observed for those smaller particles for some reactions [49], then this size-specific catalytic activity can produce an inverse TOF *versus* precatalyst concentration dependence. In structure insensitive reactions such as ours, the explanation would be straightforward: the catalytic activity per metal atom is expected to decrease as the fraction of surface sites over the total metal atoms decreases with the increasing particle size. However, it has previously never been unequivocally demonstrated. Herein we report for the first time the inverse correlation between the catalytic activity and the size of nanoparticles by having measured both quantities accurately. The TOF value of Rh(0)/nanoSiO$_2$ in hydrogen generation from the methanolysis of AB decreases as the particle size of the rhodium(0) nanoparticles increases with the increasing initial concentration of rhodium (Fig. 6f and Fig. 8b). However, when the TOF values are corrected for the number of rhodium atoms on the surface of nanoparticle (Table 1) the inverse dependence of the catalytic activity on the size of nanoparticles disappears, as the corrected TOF values are similar to each other within the experimental error. The disappearance of inverse dependence for the corrected TOF values is also a compelling evidence that the inverse relation between the catalytic activity and the concentration of rhodium is indeed a size issue.

The hydrogen generation rate (Table 1) was plotted *versus* the initial concentration of rhodium, both axes in logarithmic scale (The inset in Fig. 8a). This plot gives a straight line with a slope of $0.98 \approx 1.0$ indicating that the methanolysis of AB catalysed by Rh(0)/nanoSiO$_2$ is first order with respect to rhodium concentration. It is noteworthy that the hydrogen generation proceeds almost linearly after the induction period in each experiment, without being changed in the course of reaction; therefore, the methanolysis reaction is most likely zero order with respect to the AB concentration.

Activation parameters for the nucleation and autocatalytic surface growth of the rhodium(0) nanoparticles on the surface of nanosilica as well as for the catalytic methanolysis of AB catalysed by Rh(0)/nanoSiO$_2$ could be obtained from the temperature dependent kinetic data. Fig. 9a shows the plots of mole H_2 evolved per mole of AB *versus* time for the methanolysis of AB starting with 0.49 mM Rh catalyst (1.0 wt.% Rh, 50 mg Rh^{2+}/nanoSiO$_2$) plus 200 mM AB substrate at various temperatures. The experimental data curve-fit well to the two-step mechanism yielding the rate constants k_1 of the slow, continuous nucleation ($P \rightarrow Q$) and k_2 of the autocatalytic surface growth ($P + Q \rightarrow 2Q$) for the formation of rhodium(0) nanoparticles catalyst during the methanolysis of AB [33]. The rate constants k_2 and k_1 as well the k_2/k_1 ratio are listed in Table 2. The large value of k_2/k_1 ratio is indicative of a high level kinetic control in the formation of rhodium(0) nanoparticles from the reduction of rhodium(II) precursor in the presence of silica nanopowder at any temperature in the range 20–40 °C [34]. Activation energy for the nucleation and autocatalytic surface growth could be determined from the Arrhenius plots by using the values of rate constants k_1 and k_2 at various temperatures in Fig. 9b and c, respectively: $E_a = 79 \pm 5$ kJ/mol for the nucleation and $E_a = 49 \pm 2$ kJ/mol for the autocatalytic surface growth. Activation energy values give an idea on the energy barrier for the slow nucleation and autocatalytic surface growth of metal(0) nanoparticles catalyst.

The hydrogen generation rate was calculated from the slope of the linear part of each plot in Fig. 9a. The reaction rate con-

Table 2
The rate constants k_1 of the slow, continuous nucleation,P → Q, and k_2 of the autocatalytic surface growth, P + Q → 2Q, for the formation of rhodium(0) nanoparticles catalyst from the reduction of rhodim(II) ions during the methanolysis of AB, hydrogen generation rates, k_{obs} values, turnover frequency (TOF) values, and the TOF values corrected for the number of rhodium atoms on the surface of nanoparticles for the methanolysis of AB starting with [AB] = 200 mM and [Rh] = 0.49 mM at different temperatures.

Temperature (°C)	k_1 (min^{-1})	k_2 (M^{-1} min^{-1})	k_2/k_1	H_2 generation rate (mmol H_2 min^{-1})	k_{obs} (mol H_2 molRh^{-1} s^{-1})	TOF (min^{-1})	$TOF_{corrected}$ (min^{-1})
20	$2.03 \times 10^{-2} \pm 1.34 \times 10^{-3}$	84.9 ± 2.2	4.19×10^3	0.77	1.39	92	325
25	$3.03 \times 10^{-2} \pm 2.45 \times 10^{-3}$	121.3 ± 3.9	4.01×10^3	1.17	2.46	147	519
30	$6.44 \times 10^{-2} \pm 4.36 \times 10^{-3}$	160.7 ± 5.2	2.50×10^3	1.70	4.10	246	869
35	$1.03 \times 10^{-1} \pm 6.39 \times 10^{-3}$	229.0 ± 7.1	2.22×10^3	2.57	6.23	380	1343
40	$1.55 \times 10^{-1} \pm 8.54 \times 10^{-3}$	310.7 ± 10.0	2.01×10^3	3.63	7.66	460	1625

Table 3
Catalytic activity of metal(0) catalysts used for the catalytic methanolysis of ammonia borane and the activation energy of the catalytic methanolysis of ammonia borane.

Catalyst	TOF (mol H_2 mol $catalyst^{-1}$ min^{-1})	Activation energy, E_a (kJ mol^{-1})	Ref.
$RhCl_3$	100	–	[8]
$RuCl_3$	150	–	[8]
$CoCl_2$	3.7	–	[8]
$NiCl_2$	2.9	–	[8]
$PdCl_2$	1.5	–	[8]
Pd/C	1.9	–	[8]
Nano Cu_2O	0.2	–	[13]
Nano Cu@Cu_2O	0.16	–	[13]
PVP-stabilized Ni	12.1	62 ± 2	[14]
PVP-stabilized Pd	22.3	35 ± 2	[15]
PVP-stabilized Ru	47.7	58 ± 2	[16]
Co-Co_2B	7.5	–	[17]
Ni-Ni_3B	5.0	–	[17]
Co-Ni-B	10.0	–	[17]
Zeolite confined Rh	30.0	40 ± 2	[18]
MMT stabilized Ru	90.9	23.8	[19]
$Co_{48}P_{52}$ /C	27.7	25.5	[20]
mesoporous CuO	2.41	34.2 ± 1.2	[21]
Cu-Cu_2O-CuO/C	24.0	67.9	[22]
Rh(0)/nanoSiO_2	168 (506)[a]	62 ± 2	This study

[a] The value corrected for the number of rhodium atom on the surface of nanoparticle.

stants k_{obs} and the TOF values were calculated from the hydrogen generation rates at various temperatures (Table 2). The increase in the temperature expectedly enhances the rate of hydrogen generation from the methanolysis of AB. It is noteworthy that also TOF value increases with increasing temperature reaching the remarkable value of 460 min^{-1} (1625 min^{-1} corrected for the number of rhodium atoms on the surface of nanoparticle) in hydrogen generation from the methanolysis of AB at 40 °C catalysed by Rh(0)/nanoSiO_2 nanoparticles. The apparent activation parameters were calculated by using Arrhenius [50] and Eyring [51] plots given in Fig. 9d and e, respectively: the activation energy $E_a^{app} = 62 \pm 2$ kJ/mol, the activation enthalpy $\Delta H^{\neq,app} = 59 \pm 2$ kJ/mol, and the activation entropy $\Delta S^{\neq,app} = -18 \pm 4$ J/mol K. The activation energy for the hydrogen generation from the methanolysis of AB catalyzed by Rh(0)/nanoSiO_2 is comparable to the literature values reported for the methanolysis of AB using different metal containing catalyst (Table 3).

The catalytic lifetime of nanosilica stabilized rhodium(0) nanoparticles was measured by determining the total turnover number provided by nanoparticles in hydrogen generation from the methanolysis of AB at room temperature before their deactivation. Such a life time experiment was performed starting with 10 mL suspension containing 0.99 mM Rh (50.0 mg Rh(0)/nanoSiO_2, 2.0 wt.% Rh,) and 400 mM AB at 25.0 ± 0.5 °C (Fig. 10). When expected amount of H_2 gas liberated, a new batch of AB was added into the reaction flask and hydrogen generation was followed. This procedure was iterated until no more gas evolution was observed.

As depicted in Fig. 10, the nanosilica stabilized rhodium(0) nanoparticles provide 10,000 turnovers in hydrogen generation from the methanolysis of AB at 25.0 ± 0.5 °C before deactivation. The initial turnover frequency (TOF) value is 133 min^{-1} (516 min^{-1} the value corrected for the number of rhodium atom on the surface of nanoparticle) for nanosilica stabilized rhodium(0) nanoparticles in hydrogen generation from the methanolysis of AB at 25.0 ± 0.5 °C. Note that Rh(0)/nanoSiO_2 provides the highest TOF value ever reported for methanolysis of AB using rhodium catalyst such as $RhCl_3$ (TOF = 100 min^{-1}) [8], zeolite confined rhodium(0) nanoparticles (TOF = 30 min^{-1}) [18].

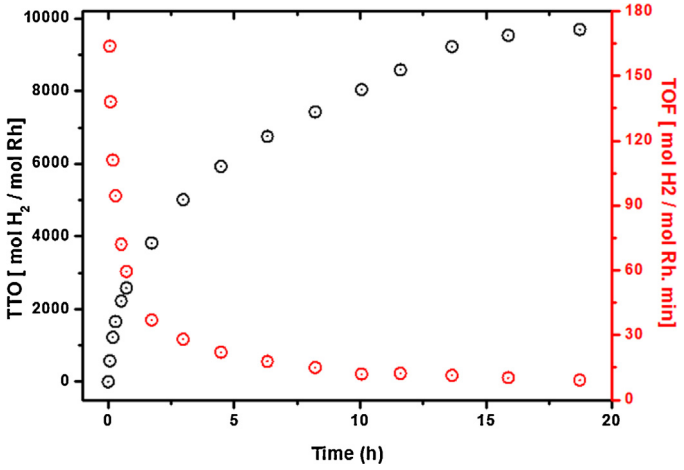

Fig. 10. Plot of total turnover number (TTO) or turnover frequency *versus* time for the methanolysis of AB with 10 mL solution of 0.99 mM Rh (50.0 mg Rh(0)/nanoSiO_2, 2.0 wt.% Rh,) and 400 mM AB (for each run) at 25.0 ± 0.5 °C.

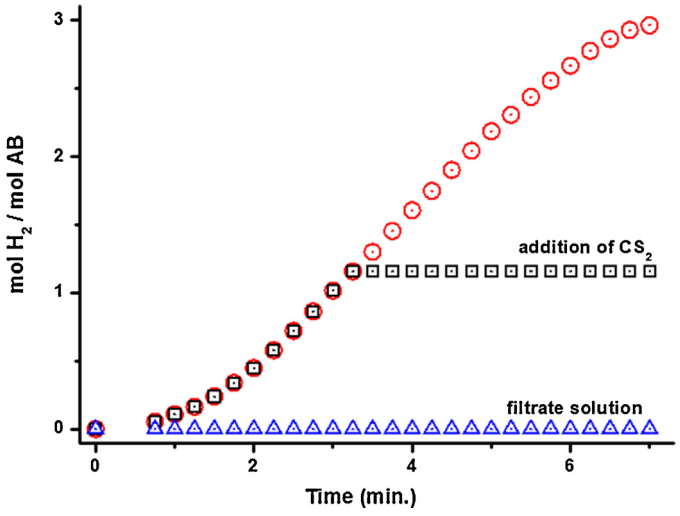

Fig. 11. Plots of mole H_2 evolved per mole of AB *versus* time for the methanolysis of 200 mM AB catalyzed by Rh(0)/nanoSiO$_2$ (0.49 mM Rh, 1.0 wt.% Rh(0)/nanoSiO$_2$) with (square, □) and without (circle, ○) addition of 0.2 equiv. CS_2, and (triangle, Δ) the filtrate solution obtained from filtration of active catalyst after methanolysis of AB at 25.0 ± 0.5 °C.

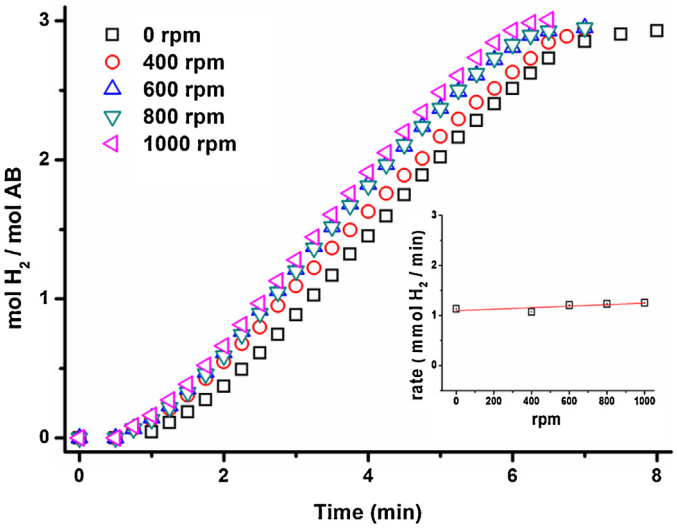

Fig. 12. Plots of mole H_2 evolved per mole of ammonia borane *versus* time for the catalytic methanolysis of AB starting with 200 mM AB and 0.49 mM Rh (50 mg Rh^{+2}/nanoSiO$_2$, 1.0 wt.% Rh) in 10 mL methanol at 25.0 ± 0.5 °C at different stirring rate. The inset shows the plot of hydrogen generation rate *versus* the stirring rate.

3.4. Carbon disulfide (CS_2) poisoning as heterogeneity test for Rh(0)/nanoSiO$_2$ in the methanolysis of AB

The heterogeneity of nanosilica stabilized rhodium(0) nanoparticles was checked by performing a CS_2 poisoning experiment. Due to the strong binding of poison to the metal center, the access of the substrate to the active site is blocked by poison [52,53]. In our poisoning experiment, after the liberation of 40% hydrogen from methanolysis of AB (200 mM) catalyzed by 0.49 mM Rh, when the catalytically active rhodium(0) nanoparticles were certainly formed, 0.20 equivalent CS_2 per mole of rhodium was swiftly injected to reaction flask, whereby the activity of nanosilica stabilized rhodium(0) nanoparticles was inhibited and hydrogen generation from the methanolysis of AB ceased immediately (Fig. 11). The complete cessation of catalytic methanolysis of AB upon CS_2 addition is a compelling evidence for the heterogeneity of nanosilica stabilized rhodium(0) nanoparticles in the methanolysis of AB.

3.5. Leaching test for Rh(0)/nanoSiO$_2$

A control experiment was also performed in order to show that hydrogen generation from the methanolysis of AB is completely ceased by the removal of catalytically active Rh(0)/nanoSiO$_2$ from reaction flask. A methanolysis experiment was performed starting with 200 mM AB plus 50 mg Rh^{+2}/nanoSiO$_2$ (1.0% wt. Rh, [Rh] = 0.49 mM) in 10 mL methanol at 25.0 ± 0.5 °C. After the completion of catalytic methanolysis of AB, the reaction flask was opened under inert gas atmosphere; reaction solution was filtered to remove Rh(0)/nanoSiO$_2$, effectively. Filtrate was transferred into another reaction flask. A new batch of 200 mM AB was added to the reaction flask, hydrogen generation was monitored at 25.0 ± 0.5 °C. Filtrate solution exhibits no catalytic activity in the methanolysis of AB (Fig. 11). The results of the leaching test confirms the retaining of rhodium(0) nanoparticles within the nanosilica matrix (no rhodium passes into solution). It can also be concluded that Rh(0)/nanoSiO$_2$ are kinetically competent and heterogeneous catalyst in the methanolysis of AB. It is noteworthy that accurate measurement of the catalytic activity of isolated solid materials is not possible because of the notable materials loss during the isolation and redispersion.

3.6. Establishment of that the Rh(0)/nanoSiO$_2$ catalyzed methanolysis of AB is in the kinetic regime

An important question to answer is whether the hydrogen generation from the methanolysis of AB is in the kinetic regime [54]. To answer this question, a control experiment was performed starting with 200 mM AB and 0.49 mM Rh (50 mg Rh^{+2}/nanoSiO$_2$, 1.0 wt.% Rh) in 10 mL methanol at 25.0 ± 0.5 °C by varying the stirring rate. The results of the control experiment are given in Fig. 12 which shows that stirring rate has essentially no effect on the rate of hydrogen generation from the methanolysis of AB at 25.0 ± 0.5 °C. This is a classic simple, but convincing, piece of evidence for the reaction being in the kinetic regime, not under the mass transfer limitations [55]. The observation that the hydrogen generation rate is independent of the stirring rate can be ascribed to small particle size of support (smaller than 12 nm). Different from the other supported catalysts, Rh(0)/nanoSiO$_2$ doesn't precipitate when left in solution and remains as suspension for weeks. Thus, the rhodium(0) nanoparticles on the surface of small sized nanosilica are readily accessible by the substrate molecules, even in a nonstirred solution. Note that all the experiments in this study were performed under stirring at 1000 rpm.

4. Conclusions

The main finding and insights from this work can be summarized as follows;

a The nanosilica stabilized rhodium(0) nanoparticles are *in situ* generated from reduction of rhodium(II) ions impregnated on the surface of porous nanosilica during the methanolysis of AB at room temperature.
b The reduction of rhodium(II) ions impregnated on nanosilica during the methanolysis of AB leads to the formation of rhodium(0) nanoparticles in tunable size depending on the initial concentration of rhodium. The mean particle size of rhodium(0) nanoparticles increases with the increasing initial concentration of rhodium precursor used. This observation indicates that the metal nanoparticles size can be tuned by varying the initial concentration of metal precursor complex.

c The use of hydrogen generation from the methanolysis of AB as reporter reaction provides valuable insights to the formation kinetics of rhodium(0) nanoparticles. The observation of a sigmoidal dehydrogenation curve and its curve-fit to the slow, continuous nucleation (rate constant k_1), followed by autocatalytic surface growth (rate constant k_2) kinetics are very strong evidence for the formation of rhodium(0) nanoparticles catalyst from the reduction of rhodium(II) ions in the presence of AB reducing agent.

d The high values of k_2/k_1 ratio obtained in the experiments with different rhodium concentrations and at various temperatures are indicative of a high level kinetic control in the formation of rhodium(0) nanoparticles from the reduction of rhodium(II) precursor impregnated on silica nanopowder.

e Using the values of rate constants k_1 and k_2 at various temperatures enables us to determine the activation energies for the slow, continuous nucleation and autocatalytic surface growth of rhodium(0) nanoparticles to be 79 ± 5 kJ/mol and 49 ± 2 kJ/mol, respectively.

f Nanosilica stabilized rhodium(0) nanoparticles are highly active and long lived catalyst in hydrogen generation from the methanolysis of AB providing a release of 3.0 equivalent of H_2 per mole of AB with an exceptional initial turnover frequency of 133 min^{-1} (516 min^{-1} when corrected for the number of rhodium atom on the surface of nanoparticle) which is the highest value ever reported for rhodium catalysts, and 10,000 turnovers in hydrogen generation from the methanolysis of AB at 25.0 ± 0.5 °C before deactivation.

g An inverse dependence of turnover frequency *versus* the initial concentration of rhodium is observed for the nanosilica stabilized rhodium(0) nanoparticles in hydrogen generation from the methanolysis of AB. This inverse dependence was shown to be due the increasing size of rhodium(0) nanoparticles with the increasing initial concentration of metal precursor.

h The kinetic study reveals that methanolysis is first order with respect to the catalyst concentration and zero order with respect to substrate concentration.

i Carbon disulfide poisoning experiment and filtration test showed that nanosilica stabilized rhodium(0) nanoparticles are kinetically competent catalyst and the catalytic methanolysis of AB is heterogeneous.

j One-pot preparation, high stability, and high catalytic activity of rhodium(0) nanoparticles supported on the surface of silica nanopowder make them promising candidate to be exploited as catalyst in releasing hydrogen from AB which has been considered as hydrogen storage materials for portable application systems.

Acknowledgments

Partial support by Turkish Academy of Sciences and TUBITAK for a scholarship to DÖ is gratefully acknowledged.

References

[1] S. Satyapal, J. Petrovic, G. Thomas, Sci. Am. 296 (2007) 80–87.
[2] M.S. Dresselhaus, I.L. Thomas, Nature 414 (2001) 332–337.
[3] B. Sakintuna, F. Lamari-Darkrim, M. Hirscher, Int. J. Hydrog. Energy 32 (2007) 1121–1140.
[4] E.K. Stefanakos, D.Y. Goswami, S.S. Srinivasan, J.T. Wolan, In Environmentally Conscious Alternative Energy Production, JohnWiley & Sons, New York, 2007.
[5] L. Schlapbach, A. Züttel, Nature 414 (2001) 353–358.
[6] F. Hausdorf, F. Baitlow, G. Wolff, F. Mertens, Int. J. Hydrog. Energy 33 (2008) 608–614.
[7] T. Hügle, M.F. Kühnel, D. Lentz, J. Am. Chem. Soc. 131 (2009) 7444–7446.
[8] P.V. Ramachandran, P.D. Gagare, Inorg. Chem. 46 (2007) 7810–7817.
[9] F.H. Stephens, V. Pons, R.T. Baker, Dalton Trans. 25 (2007) 2613–2626.
[10] T.B. Marder, Angew. Chem. Int. Ed. 46 (2007) 8116–8118.
[11] M. Zahmakıran, S. Özkar, Top. Catal. 56 (2013) 1171–1183.
[12] A. Brockman, Y. Zheng, J. Gore, Int. J. Hydrog. Energy 35 (2010) 7350–7356.
[13] S.B. Kalidindi, U. Sanyal, B.P. Jagirdar, Phys. Chem. Chem. Phys. 10 (2008) 5870–5874.
[14] D. Özhava, N.Z. Kılıçaslan, S. Özkar, Appl. Catal. B Environ. 162 (2015) 573–582.
[15] H. Erdogan, Ö. Metin, S. Özkar, Phys. Chem. Chem. Phys. 44 (2009) 10519–10525.
[16] H. Erdogan, Ö. Metin, S. Özkar, Catal. Today 170 (2011) 93–98.
[17] S.B. Kalidindi, A.A. Vernekar, B.R. Jagirdar, Phys. Chem. Chem. Phys. 11 (2009) 770–775.
[18] S. Çalışkan, M. Zahmakıran, S. Özkar, Appl. Catal. B Environ. 93 (2010) 387–394.
[19] H.B. Dai, X.D. Kang, P. Wang, Int. J. Hydrog. Energy 35 (2010) 10317–10323.
[20] D. Sun, V. Mazumder, Ö. Metin, S. Sun, ACS Catal. 2 (2012) 1290–1295.
[21] Q. Yao, M. Huang, Z. Lu, Y. Yang, Y. Zhang, X. Chen, Z. Yang, Dalton Trans. 44 (2015) 1070–1076.
[22] M. Yurderi, A. Bulut, I.E. Ertas, M. Zahmakiran, M. Kaya, Appl. Catal. B Environ. 165 (2015) 169–175.
[23] M. Zahmakiran, S. Özkar, Nanoscale 3 (2011) 3462–3481.
[24] L. Tosheva, V.P. Valtchev, Chem. Mater. 17 (2005) 2494–2513.
[25] E. Castillejos, P.J. Debouttiere, L. Roiban, A. Solhy, V. Martinez, Y. Kihn, O. Ersen, K. Philippot, B. Chaudret, P. Serp, Angew. Chem. Int. Ed. 48 (2009) 2529–2533.
[26] M.S. El-Shall, V. Abdelsayed, A.E.R.S. Khder, H.M.A. Hassan, H.M. El-Kaderi, T.E. Reich, J. Mater. Chem. 19 (2009) 7625–7631.
[27] V. Polshettiwar, C. Len, A. Fihri, Coord. Chem. Rev. 253 (2009) 2599–2626.
[28] M.K. Richmond, S.L. Scott, H. Alper, J. Am. Chem. Soc. 123 (2001) 10521–10525.
[29] M. Zahmakıran, Y.R. Leshkov, Y. Zhang, Langmuir 28 (2011) 60–64.
[30] Y. Lin, R.G. Finke, J. Am. Chem. Soc. 116 (1994) 8335–8353.
[31] CRC Handbook of Chemistry and Physics, in: D.R. Lide, H.P.R. Frederikse (Eds.), 77th ed., CRC Press, Boca Raton, FL, 1996.
[32] M.A. Watzky, R.G. Finke, J. Am. Chem. Soc. 119 (1997) 10382–10400.
[33] J.A. Widegren, J.D. Aiken, S. Özkar, R.G. Finke, Chem. Mater. 13 (2001) 312–324.
[34] M.A. Watzky, R.G. Finke, Chem. Mater. 9 (1997) 3083–3095.
[35] Y. Baer, P.F. Heden, J. Hedman, M. Klasson, C. Nordling, K. Siegbahn, Phys. Scr. 1 (1970) 55–65.
[36] V. Mevellec, A. Nowicki, A. Roucoux, C. Dujardin, P. Granger, E. Payen, K. Philippot, New J. Chem. 30 (2006) 1214–1219.
[37] T.L. Barr, J. Phys. Chem. 82 (1978) 1801–1810.
[38] M. Peuckert, Surf. Sci. 141 (1984) 500–514.
[39] P.A. Umpierre, E. de Jesus, J. Dupont, ChemCatChem 3 (2011) 1413–1418.
[40] M. Boudart, Chem. Rev. 95 (1995) 661–666.
[41] F.K. Shmidt, L.O. Nindakova, B.A. Shainyan, V.V. Saraev, N.N. Chipanina, V.A. Umanetz, J. Mol. Catal. A Chem. 235 (2005) 161–172.
[42] B.A. Steinhoff, S.R. Fix, S.S. Stahl, J. Am. Chem. Soc. 124 (2002) 766–767.
[43] R.A. Sanchez-Delgado, A. Andriollo, J. Puga, G. Martin, Inorg. Chem. 26 (1987) 1867–1870.
[44] M.T. Reetz, J.G. De Vries, Chem. Commun. 14 (2004) 1559–1563.
[45] A.H.M. De Vries, J.M.C.A. Mulders, J.H.M. Mommers, H.J.W. Henderickx, J.G. De Vries, Org. Lett. 5 (2003) 3285–3288.
[46] K.M. Doll, R.G. Finke, Inorg. Chem. 43 (2004) 2611–2623.
[47] J.M. Malin, H.E. Toma, E. Giesbrecht, J. Chem. Educ. 54 (1977) 385–387.
[48] X. Zhou, W. Xu, G. Liu, D. Panda, P. Chen, J. Am. Chem. Soc. 132 (2010) 138–146.
[49] M.A. Watzky, E.E. Finney, R.G. Finke, J. Am. Chem. Soc. 130 (2008) 11959–11969.
[50] K.J. Laidler, Chemical Kinetics, third ed., Harper & Row Publishers, New York, 1987.
[51] H. Eyring, J. Chem. Phys. 3 (1935) 107–115.
[52] B.J. Hornstein, J.D. Aiken, R.G. Finke, Inorg. Chem. 41 (2002) 1625–1638.
[53] M.N. Vargaftik, V.P. Zargorodnikov, I.P. Stolarov, I.I. Moiseev, D.I. Kochubey, V.A. Likholobov, A.L. Chuvilin, K.I. Zamaracv, J. Mol. Catal. 53 (1989) 315–348.
[54] F. Notheisz, Á. Zsigmond, M. Bartók, Z. Szegletes, G.V. Smith, App. Catal. A Gen. 120 (1994) 105–114.
[55] R.J. Madon, M. Boudart, Ind. Eng. Chem. Fundam. 21 (1982) 438–447.